

Characterization and interpretation of the quantum efficiencies of multilayer semiconductor detectors using a new theory

T. Cho,^{a*} M. Hirata,^a J. Kohagura,^a Y. Sakamoto,^a T. Okamura,^a T. Numakura,^a R. Minami,^a Y. Nishizawa,^a T. Sasuga,^a T. Tamano,^a K. Yatsu,^a S. Miyoshi,^a S. Tanaka,^b K. Sato,^c Y. Saitoh,^c K. Hirano^d and H. Maezawa^d

^aPlasma Research Centre, University of Tsukuba, Ibaraki 305, Japan, ^bKyoto University, Kyoto 606, Japan, ^cSII, Japan, and ^dPhoton Factory, Institute of Material Structure Science, High Energy Accelerator Research Organization, Ibaraki 305, Japan. E-mail: tcho@prc.tsukuba.ac.jp

(Received 4 August 1997; accepted 6 January 1998)

On the basis of a new theory of semiconductor X-ray detector response, a new type of multilayer semiconductor detector was designed and developed for convenient energy analyses of intense incident X-ray flux in a cumulative-current mode. Another anticipated useful property of the developed detector is a drastic improvement in high-energy X-ray response ranging over several hundred eV. The formula for the quantum efficiency of multilayer semiconductor detectors and its physical interpretations are proposed and have been successfully verified by synchrotron radiation experiments at the Photon Factory. These detectors are useful for data analyses under strong radiation-field conditions, including fusion-plasma-emitting X-rays and energetic heavy-particle beams, without the use of high-bias applications.

Keywords: semiconductor detectors; X-ray detectors; multilayer detectors.

1. Introduction

Compact-sized X-ray detectors having a high response over a wide energy range (from 100 eV to several hundred keV) have recently been required in association with developments in fusion-oriented plasma investigations (Alper *et al.*, 1997). In these experiments, energy-resolved X-ray tomographic reconstruction data provide important information on electron behaviour in a strong ambient magnetic field.

A high degree of immunity to magnetic fields permits semiconductor detectors to be used in plasma experimental devices, with magnetic fields of several tesla and vacuum environments of the order of 10^{-9} torr (Cho *et al.*, 1990, 1992a). This provides remarkable advantages compared with the use of detectors which utilize avalanche electrons for the signal outputs, including photomultipliers and microchannel plates (Hirata *et al.*, 1990).

Despite the merits of semiconductor detectors, their quantum efficiency begins to decrease from around 10 keV when commercially available ~ 500 μm -thick photodiodes are employed. In this article, newly designed multilayer photodiode-type semiconductor detectors for wider X-ray energy diagnostics are proposed. This new type of detector is also applicable for use in simultaneous observations of multi-energy-resolved X-ray

tomography measurements using the combined signal outputs from each detector layer (see §3 and §4).

The detection characteristics are investigated using synchrotron radiation at the Photon Factory of the High Energy Accelerator Research Organization; the results are interpreted using our recently proposed theory on the X-ray energy response of a semiconductor detector (Cho *et al.*, 1992b, 1994). This theory solved a recent confusing problem (Wenzel & Petraso, 1988) where the conventionally utilized theory (Price, 1964) of semiconductor X-ray energy response was found to be invalid. A theoretical formula for the quantum efficiency of such a unique multilayer semiconductor detector is given using our theory.

2. Experimental apparatus

The multilayer semiconductor X-ray detector is characterized using intense synchrotron radiation at the Photon Factory. X-rays ranging from 5 to 20 keV are monochromated and changed automatically using a computer-controlled double-crystal Si(111) monochromator with an energy resolution of a few eV (beamline 15C) (Cho *et al.*, 1992c; Hirata *et al.*, 1990).

The detector is placed on a computer-controlled adjustable-position system having a positional reproducibility within an accuracy of 0.5 μm and 0.005° on the detector surface, along with a goniometric control within 0.002° , in order to realize a parallel and a perpendicular X-ray injection to the diode surface. The shape of the X-ray beam (0.30×3.00 mm) is checked using a microstrip semiconductor detector having 520 channels on a $10 \text{ mm} \times 5.2 \text{ mm} \times 300 \mu\text{m}$ silicon wafer with a 10 μm width per channel (Kohagura *et al.*, 1995).

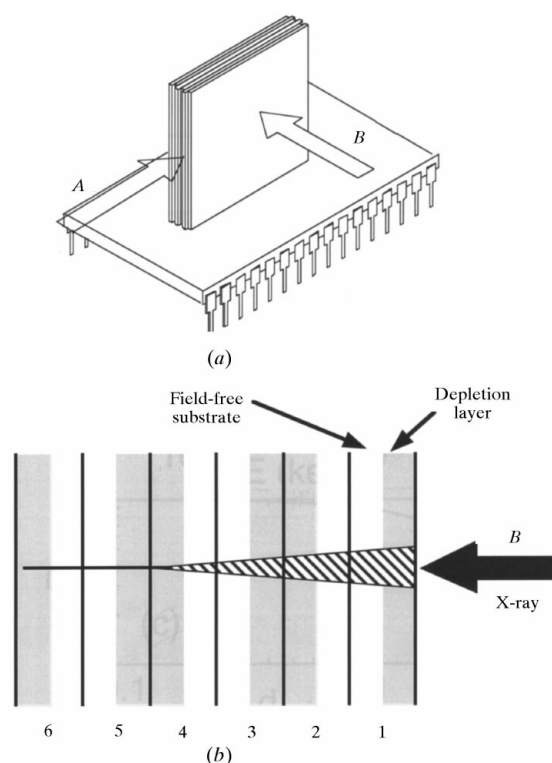


Figure 1
(a) Schematic drawing of a new multilayer semiconductor X-ray detector. X-ray injection directions A and B are shown. (b) A detailed cross section, viewed from the A direction, is shown with an absorbed X-ray beam (hatched).

The specifications for two types of multilayer detectors are as follows. Figs. 1(a) and 1(b) show schematic drawings of the six-layer detector. Each layer is essentially a p-n junction photodiode; this diode unit has a wafer thickness $d_{\text{waf}} = 525 \mu\text{m}$ and a $10 \times 10 \text{ mm}$ active area. Another multilayer detector is composed of four layers with $d_{\text{waf}} = 300 \mu\text{m}$ and a $10 \times 10 \text{ mm}$ active area.

3. Characterization of the multilayer detectors

Fig. 2(a) shows quantum efficiency normalized by the incident photon energy, η/E , of the multilayer detector with four layers. In this case, parallel X-ray injection (direction A in Fig. 1a) along the wafer surfaces is employed.

The output signals from the multilayer detector, I_{ML} , are normalized by the I_0 signals to obtain the energy response for a unit incident X-ray flux. The remarkable feature of a flat response ranging from 10 to 20 keV is achieved and is calculated to be maintained up to 30 keV, even though η/E for a one-layer photodiode under commonly utilized X-ray injection conditions (injection in direction B in Fig. 1a) begins to decrease beyond about 7 keV (the solid curve in Fig. 2b).

For a cubic-shaped $10 \times 10 \times 10 \text{ mm}$ multilayer detector, such a flat response is shown by the dashed curve (d-10) in Fig. 2(b). The

cubic-shaped configuration with X-ray beam injection at the centre of the detector is chosen and Compton effects are included in the calculations. Our four-layer detector is a prototype of this cubic-shaped detector. If a $100 \times 100 \times 100 \text{ mm}$ cubic detector is made using photodiodes having an active area of $100 \times 100 \text{ mm}$, then an almost flat response up to $\sim 0.4 \text{ MeV}$ is anticipated, as shown by the dotted curve (d-100) in Fig. 2(b). For reference, the solid curve represents the response of the first front layer. The values of R in Fig. 2(c) will be discussed in §4.

A slight decrease in the low-energy side (Fig. 2a) is interpreted by the existence of a $10 \mu\text{m}$ -thick dead layer. Such a curve is quantitatively understandable if the diffusion effects from the edge region to the active area are taken into account. This will be minimized by improvement of the location of the electrode shape.

Compared with conventional single-crystal detectors, one of the advantages of this multilayer-structured detector is that there is no need for the kV-order biasing employed for a normal 10 mm-thick single-crystal detector. A supply of only a few to some tens of volts is sufficient for operation of the multilayer detector. From the viewpoint of avoiding a detector breakdown caused by fusion-produced neutron or high-energy heavy-ion damage to the detector, such a low-bias operation provides a significant advantage.

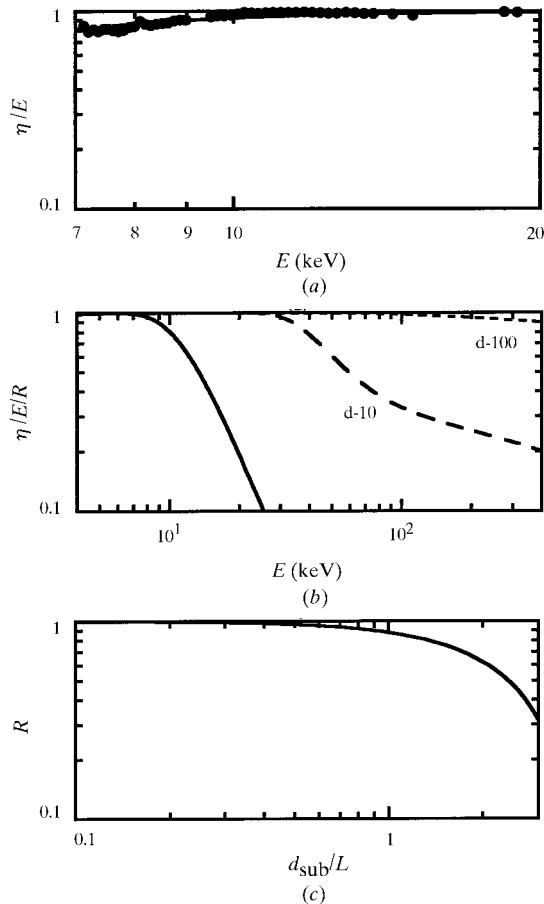


Figure 2

(a) The X-ray energy response of the four-layer detector for A-direction injection (see Fig. 1a). The curve is calculated using a $10 \mu\text{m}$ -thick dead layer and $R = 1$. (b) Quantum efficiencies η/E divided by R for B-direction injection for the first front layer of the multilayer detector and for newly designed multilayer detectors having wafer sizes $10 \times 10 \text{ mm}$ (d-10) and $100 \times 100 \text{ mm}$ (d-100). (c) The diffusion effect R on η/E is calculated as a function of d_{sub}/L . Here, $L = 100 \mu\text{m}$ and $d_{\text{waf}} = 300 \mu\text{m}$.

4. The formula and its physical interpretation for the quantum efficiency of a multilayer detector using a new theory of semiconductor X-ray response

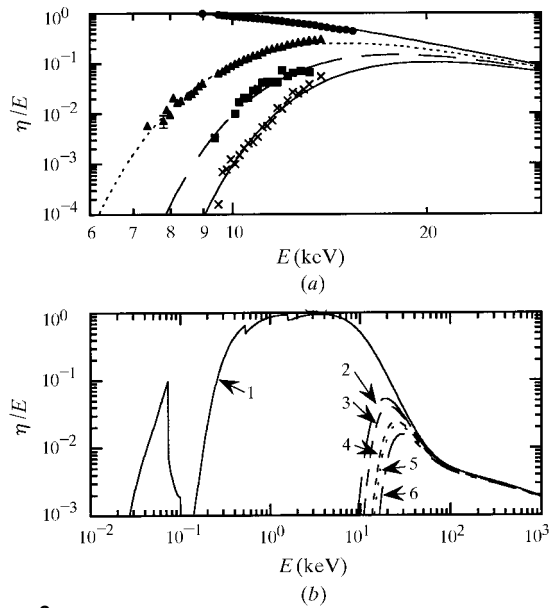
Collimated X-rays in a rectangular shape with a width of nd_{waf} (n being an integer) are utilized for the evaluation of the quantum efficiencies of multilayer detectors for side X-ray injection (direction A in Fig. 1a). Charges produced by the X-ray beam injected into a depletion layer are completely collected by an electrode with an efficiency of 100%. On the other hand, charges produced in a field-free substrate partially diffuse into a depletion layer, and are then quickly collected by an electrode (Cho *et al.*, 1992b, 1994). The collection rate, R , is physically determined from the fraction of the charges which safely reach a depletion layer without charge recombinations with impurity-ion centres in the substrate region. This process is quantitatively characterized by the diffusion length L (Hopkinson, 1987; Cho *et al.*, 1992b, 1994).

Our new theoretical formula (Cho *et al.*, 1994) for the quantum efficiency of a semiconductor X-ray detector is applicable to the X-ray response of a multilayer detector in such a configuration. X-rays injected into either a depletion layer or a field-free substrate produce charges $s(z)$ at a depth z of a magnitude $s(z) = I_0(E/\varepsilon)\mu\rho\exp(-\mu\rho z)$, where ε stands for the energy required to create an electron-hole pair, and μ and ρ denote the silicon mass-absorption coefficient and mass density, respectively.

For the total efficiency, the collection efficiencies in both regions are multiplied by the charge-production ratios, d_{dep} and d_{sub} (namely, the ratio of the depletion-layer incident X-ray area to the substrate-region area), respectively. According to the above discussion, R is described as

$$R = 1 - (L/d_{\text{waf}})[(d_{\text{sub}}/L) - 1 + \exp(-d_{\text{sub}}/L)].$$

In fully depleted operations, d_{sub} becomes zero and R becomes unity. On the other hand, in partially depleted operations, for instance, for $d_{\text{sub}}/L < 1$, R is anticipated to be greater than 0.9. Even when $d_{\text{sub}}/L = 2$ (e.g. $d_{\text{waf}} = 300 \mu\text{m}$, $d_{\text{dep}} = 100 \mu\text{m}$, and $L = 100 \mu\text{m}$), R is still maintained beyond 0.6. The values of R are plotted in Fig. 2(c).

**Figure 3**

(a) Output signals from each layer of the four-layer detector along with calculated curves for *B*-direction injection in Fig. 1(a). (b) The analogous responses of the six-layer detector (Fig. 1b). The six numbered curves correspond to the six layers in Fig. 1(b).

In Fig. 3(a), the data on the response characteristics of each of the four photodiode layers to incident X-rays in the direction *B* in Fig. 1(a) are plotted. The four fully depleted 300 μm -thick photodiodes are aligned. Good agreement between the data and

the calculations shows the availability of this configuration of the multilayer detector as an X-ray energy-resolved detector; that is, for a layer, several layers in front work as X-ray absorbers, as seen in Fig. 3(a). Therefore, the data comparison between these multilayers provides a novel method for X-ray energy analysis even if no actual filters are prepared. Similarly, Fig. 3(b) shows the response of the six-layer detector in Fig. 1(b); the detector parameters (see §2) are chosen to analyse X-ray energies around 10 keV. The six numbered curves in Fig. 3(b) correspond to the six layers in Fig. 1(b).

This gives the remarkable advantages of attaining a detector installation in a vacuum chamber without any need for access to change filters, as well as the ability to obtain energy-analysed X-ray data even if only one irreproducible shot is available.

References

- Alper, B. *et al.* (1997). *Rev. Sci. Instrum.* **68**, 778–781.
- Cho, T. *et al.* (1990). *Phys. Rev. Lett.* **64**, 1373–1376.
- Cho, T. *et al.* (1992a). *Phys. Rev. A*, **45**, 2532–2545.
- Cho, T. *et al.* (1992b). *J. Appl. Phys.* **72**, 3363–3373.
- Cho, T. *et al.* (1992c). *Phys. Rev. A*, **46**, 3024–3027.
- Cho, T. *et al.* (1994). *Nucl. Instrum. Methods. A*, **348**, 475–478.
- Hirata, M. *et al.* (1990). *Rev. Sci. Instrum.* **61**, 2566–2570.
- Hopkinson, B. R. (1987). *Opt. Eng.* **26**, 766–772.
- Kohagura, J. *et al.* (1995). *Appl. Rad. Isot.* **46**, 489–490.
- Price, W. J. (1964). *Nuclear Radiation Detection*. New York: McGraw-Hill.
- Wenzel, K. W. & Petrasso, R. D. (1988). *Rev. Sci. Instrum.* **59**, 1380–1387.